High-efficiency rotating point spread functions

Sri Rama Prasanna Pavani* and Rafael Piestun

Department of Electrical and Computer Engineering, University of Colorado, Boulder, CO 80309, USA
**Corresponding author: pavani@colorado.edu*

Abstract: Rotating point spread functions (PSFs) present invariant features that continuously rotate with defocus and are important in diverse applications such as computational imaging and atom/particle trapping. However, their transfer function efficiency is typically very low. We generate highly efficient rotating PSFs by tailoring the range of invariant rotation to the specific application. The PSF design involves an optimization procedure that applies constraints in the Gauss-Laguerre modal plane, the spatial domain, and the Fourier domain. We observed over thirty times improvement in transfer function efficiency. Experiments with a phase-only spatial light modulator demonstrate the potential of high-efficiency rotating PSFs.

OCIS codes: (110.1758)Computational imaging; (110.6880)Three-dimensional image acquisition; (110.4850)Optical transfer functions; (150.5670)Range finding; (350.4855) Optical tweezers or optical manipulation.

References and links

1. Y. Y. Schechner, R. Piestun, and J. Shamir, "Wave propagation with rotating intensity distributions," Phys. Rev. E **54**, R50–R53 (1996).
2. V. V. Kotlyar, V. A. Soifer, and S. N. Khonina, "An algorithm for the generation of laser beams with longitudinal periodicity: rotating images," J. Mod. Opt. **44**, 1409-1416 (1997).
3. R. Piestun, Y. Y. Schechner, and J. Shamir, "Propagation-invariant wave fields with finite energy," J. Opt. Soc. Am. A **17**, 294-303 (2000).
4. S. N. Khonina, V. V. Kotlyar, V. A. Soifer, M. Honkanen, J. Lautanen, and J. Turunen, "Generation of rotating Gauss–Laguerre modes with binary-phase diffractive optics," J. Mod. Opt. **46**, 227–238 (1999).
5. E. G. Abramochkin and V. G. Volostnikov, "Spiral light beams," Phys.-Usp. **47**, 1177-1203 (2004).
6. A. Y. Bekshaev, M. S. Soskin, and M. V. Vasnetsov, "Angular momentum of a rotating light beam," Opt. Comm. **249**, 367-378 (2005).
7. N. B. Simpson, L. Allen, and M. J. Padgett, "Optical tweezers and optical spanners with Laguerre-Gaussian modes," J. of Mod. Opt. **43**, 2485-2491 (1996).
8. M. P. MacDonald, L. Paterson, K. Volke-Sepulveda, J. Arlt, W. Sibbett, and K. Dholakia, "Creation and manipulation of three-dimensional optically trapped structures," Science **296**, 1101-1103 (2002).
9. R. Grimm, M. Weidemuller, and Y. B. Ovchinnikov, "Optical dipole traps for neutral atoms," Adv. At. Mol. Opt. Phys. **42**, 95-170 (2000).
10. A. Greengard, Y. Y. Schechner, and R. Piestun, "Depth from diffracted rotation," Opt. Lett. **31**, 181-183 (2006).
11. W. H. Lee, "Computer-generated holograms: techniques and applications," in *Progress in Optics*, E. Wolf, ed. (Elsevier, 1978), Chap. 3.
12. R. Piestun, B. Spektor, and J. Shamir, "Wave fields in three dimensions: analysis and synthesis," J. Opt. Soc. Am. A **13**, 1837-1848 (1996).
13. R. Piestun and J. Shamir, "Control of wave-front propagation with diffractive elements," Opt. Lett. **19**, 771-773 (1994).

1. Introduction

A delicate balance between vortex charge and the Gouy phase of a superposition of beams produces the so-called rotating beams. These beams present an intensity distribution that continuously rotates about the optical axis upon propagation [1-6]. Combinations of Gauss-Laguerre (GL) or Bessel beams have been used for optical manipulation of atoms and

#91135 - $15.00 USD Received 21 Dec 2007; revised 9 Feb 2008; accepted 20 Feb 2008; published 29 Feb 2008

microparticles [7-9]. Because each point of the transverse cross section of a rotating beam describes a spiral trajectory, they are attractive for such applications as well. The same optical elements that generate rotating beams can be used to engineer the point spread functions (PSFs) of imaging systems to rotate with defocus. These rotating PSFs significantly increase the sensitivity of depth estimation and are the foundation of a new passive ranging principle named depth from diffracted rotation [10].

The main disadvantage of existing methods to implement rotating PSF systems is low light efficiency, which makes them inappropriate for photon limited applications. In this paper, we introduce a new type of PSF named high-efficiency rotating point spread function (HER-PSF) that solves this low efficiency problem. HER-PSFs present rotating cross sections only in a predetermined region of space, which allows for additional degrees of freedom to be used towards a phase-only implementation of the transfer function and its optical element.

The rest of this paper is organized as follows: In section 2, we review the properties of rotating PSFs and establish their limitations. Section 3 introduces the new three-dimensional (3D) HER-PSFs. Section 4 describes the design methodology, and section 5 analyzes the spatial and spectral properties of HER-PSFs through modeling and experiment.

2. Rotating point spread functions

Rotating PSFs are 3D optical responses with circularly asymmetric transverse profiles that continuously rotate with defocus. They are conveniently represented in the GL modal plane as a linear superposition of GL modes that lie along a straight line [3]. A rotating PSF system can be implemented by introducing a mask that encodes the rotating PSF transfer function in the Fourier plane of a standard imaging system. For example, the superposition of modes with indices (1,1), (3,5), (5,9), (7,13), (9,17) [Fig. 1(d)] forms a useful rotating PSF transfer function as shown in Fig. 1(a) [10], where all the modes have equal energy. When such a GL superposition is implemented as the transfer function of an imaging system, the PSF of the system rotates with defocus [Fig. 2(a)].The rate of rotation, which is proportional to the slope of the straight line chosen in the GL modal plane, is maximum in the focal region. The transfer function of a rotating PSF being an eigen-Fourier transform, is a scaled version of the PSF itself.

The main disadvantage of existing rotating PSFs is their very low transfer function efficiency, which is defined as the ratio of the energy in the rotating PSF main lobes to the energy incident on the mask. This is fundamentally due to two reasons: 1) the amplitude of the rotating PSF transfer function creates highly absorptive masks, 2) part of the energy in the rotating PSF is delivered to the side lobes, which are usually not used. In the example of Fig. 1(a), the transfer function efficiency is only about 1.8%; meaning that only 1.8% of the energy incident on the rotating PSF system from a point source actually makes it to the main lobes of the PSF. Adding to - and independent of - this low efficiency problem is the encoding method of the amplitude and phase components of the transfer function that often results in unused diffraction orders, causing further loss of light. Because of the abovementioned inherent factors, current rotating PSF systems are not suitable for photon-limited applications.

3. High-efficiency rotating point spread functions

HER-PSFs solve the rotating PSFs' low efficiency problem by presenting the following key features: 1) The rotating response appears only within a limited volume instead of the whole 3D space, 2) The main features of the PSF rotate but the entire cross section is only approximately invariant within the volume of interest.

A HER-PSF specifically designed for depth estimation presents two main lobes that rotate continuously with defocus. The key advantage of this HER-PSF is that its transfer function efficiency is over 30 times higher than in the case of the exact rotating PSF. Unlike previous rotating PSFs, HER-PSFs have phase-only coherent transfer functions and hence can be implemented with non-absorbing masks. HER-PSFs are engineered using an iterative optimization procedure to have the following attributes: 1) a continuous rotation of the main

#91135 - $15.00 USD Received 21 Dec 2007; revised 9 Feb 2008; accepted 20 Feb 2008; published 29 Feb 2008

lobes with defocus within a specified range, 2) maximum energy directed towards the main lobes, and 3) the transfer function modulates only the phase (no absorption).

4. HER-PSF design by iterative optimization

It is straightforward to design a phase mask for achieving any arbitrary complex field on any one particular transverse plane [11]. In such a design, the fields in all other axial planes would be dictated by diffraction. However, in the HER-PSF design, we seek a phase mask that generates a particular intensity distribution on one transverse plane and its continuously rotated versions on the following planes. In other words, we are looking for a 2D phase mask to generate a specific 3D intensity distribution. Although a 2D mask cannot achieve any arbitrary 3D complex field, it is known that the available degrees of freedom can be optimized to obtain any arbitrary 3D intensity distribution subject to physical limitations [12]. Because of the strong constraints on the intensity of the transfer function (phase-only) and the intensity of the 3D PSF (rotating main lobes with maximum energy), the only degrees of freedom in the HER-PSF design are 1) phase of the transfer function and 2) phase of the 3D PSF. One method for achieving this could be to use the block-iterative weighted projections algorithm [12,13]. To apply this method in three dimensions, each 2D transverse slice of a desired 3D intensity distribution is applied as a constraint to the mask. A continuous 3D distribution requires a suitable axial sampling rate. In the proposed design, we substantially reduce the number of required constraints by starting with an efficient initial estimate and by iteratively enforcing constraints in three different domains; namely the GL modal plane, the spatial domain, and the Fourier domain. While the idea of optimizing a 3D optical response over a finite domain is not new, the combination of spatial, spectral, and GL plane constraints has not been attempted before.

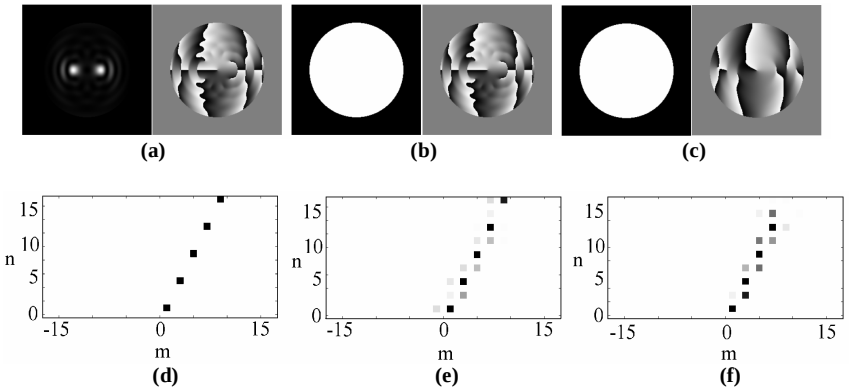

Fig. 1. Transfer functions of (a) rotating PSF, (b) HER-PSF initial estimate, and (c) HER-PSF. (d), (e), and (f) are the GL modal plane decompositions of the transfer functions in (a), (b), and (c), respectively. The transfer functions of the HER-PSF initial estimate and the HER-PSF form a cloud around the line in (d).

4.1 Initial estimate

We now describe the initial estimate that is fed into the iterative optimization algorithm. Typically, the phase of a GL mode or a GL mode superposition determines the behavior of the beam to a larger extent than its amplitude. For example, when the amplitude of a GL mode is replaced by a constant amplitude, the beam still closely resembles the original mode in the far field. Consider again the rotating PSF [Fig. 2(a)] and its transfer function [Figs. 1(a), 1(d)]. When the amplitude of the GL superposition is removed from the transfer function [Fig. 1(b)], the PSF still exhibits two main lobes that rotate continuously with defocus [Fig. 2(b)]. This seemingly surprising result can be understood by representing the transfer function in the GL modal plane. When the phase of the exact GL superposition is decomposed into its fundamental GL basis functions in the GL modal plane, it forms a cloud centered along the

#91135 - $15.00 USD Received 21 Dec 2007; revised 9 Feb 2008; accepted 20 Feb 2008; published 29 Feb 2008

same straight line as the exact superposition [Fig. 1(e)]. Since the slope of the major axis of the cloud is same as the straight line of the exact GL superposition, the rate of rotation of the new PSF remains the same. The observation that a PSF with two rotating main lobes can be formed by a cloud centered around a line in the GL modal plane relieves us from the restriction of picking modes along just one line in the GL modal plane. Thus, by merely ignoring the amplitude of the exact GL superposition, we satisfy two of the three HER-PSF attributes—phase-only transfer function and the continuous rotation of the PSF main lobes with defocus Although this PSF offers 41.9% transfer function efficiency, it is not optimal in terms of efficiency and suffers from high side lobes in the focal region. Hence, we use this phase-only transfer function as the initial estimate in our optimization procedure.

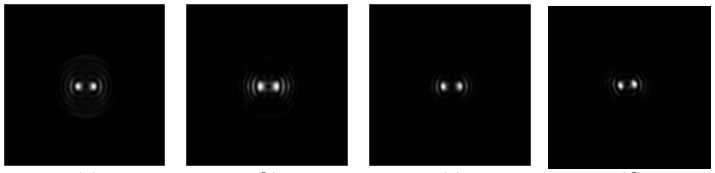

Fig. 2. Movies of different rotating PSFs: (a) Exact rotating PSF, (b) HER-PSF initial estimate, (c) HER-PSF, and (d) the experimental implementation of HER-PSF. HER-PSF has over 30 times higher efficiency than the exact rotating PSF.

4.2. Optimization constraints

The iterative optimization procedure starts with the above transfer function estimate and repeatedly enforces constraints specifically designed for achieving PSF rotation, maximum energy in the PSF main lobes, and a phase-only transfer function.

For enforcing PSF rotation, we decompose the transfer function into GL modes and multiply the GL modal plane decomposition by a weight function to boost the modes that lie on a cloud around the line defining the exact rotating PSF. The expression for this cloud weight function is obtained from a function $d(m,n)$ defined as,

$$d(m,n) = \prod_{k=1}^{N} [(m-m_k)^2 + (n-n_k)^2]^p , \qquad (1)$$

where m and n are the indices of the GL modal plane, m_k and n_k are the m and n indices of the k^{th} GL mode along the rotating PSF line, N is the number of modes selected along the rotating PSF line, and p is a parameter that determines the width of the cloud. The weight function $w_{gl}(m,n)$ is directly obtained from $d(m,n)$ as $w_{gl}(m,n) = \max[d(m,n)] - d(m,n)$.

To maximize the energy in the main lobes of the entire 3D PSF, we apply constraints to boost the PSF main lobes at nine defocus values spanning the $[-\pi/2, \pi/2)$ rotation range of the 3D PSF. Specifically, we compute the coherent PSF for a particular defocus value and multiply it by a weight function designed to boost the main lobes at that particular defocus. The weight function consists of two spatially separated Gaussians whose locations and widths are the same as those of the main lobes of the rotating PSF. Due to the continuous rotation of the rotating PSF along with varying scale, the spatial width and the locations of its main lobes change continuously with defocus. Consequently, the weight functions also need to change for different defocus values. We construct nine different weight functions for the nine different slices of the 3D PSF. The number of axial constraints needed here (nine) is not large because of the fact that the constraint in the GL modal plane already ensures continuous rotation.

The final constraint is to enforce that the transfer function is a phase-only function in the Fourier domain. Even though the initial estimate was a phase-only transfer function, the modal plane and the spatial domain constraints affect the transfer function to include amplitude modulation. However, because the preceding two constraints only boosted already existing features of the PSF, the modified transfer function is close to being phase-only.

#91135 - $15.00 USD Received 21 Dec 2007; revised 9 Feb 2008; accepted 20 Feb 2008; published 29 Feb 2008

Therefore, the third constraint enforces the transfer function to be phase-only by replacing its amplitude with a constant amplitude function.

As is customary in optimization algorithms, there is some freedom in the selection of the weight functions. The selections described above were particularly efficient in this case.

5. Results

The above three constraints were repeatedly enforced in an optimization loop. After a few iterations, a HER-PSF mask that approximately satisfies all three of its desired attributes is obtained. We monitor the desired attributes at the end of each of the iterations. Specifically, we check if the modes form a cloud in the GL modal plane, if the peak intensity of the main lobes is increasing, and if the mask is phase-only. The phase-only attribute is quantified by computing the mask's transparency (T), defined as,

$$T = \sum_x \sum_y \left| H_i(x,y) \right| \Big/ \sum_x \sum_y C(x,y), \tag{2}$$

where $H_i(x,y)$ is the complex mask immediately before enforcing the phase-only constraint and $C(x,y)$ represents a clear aperture of the same size.

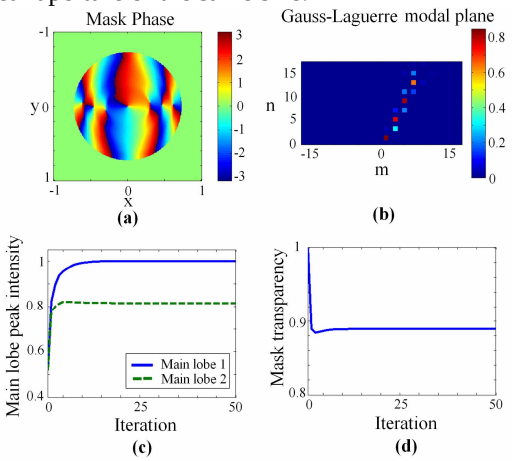

Fig. 3. Movie of the evolutions of (a) mask phase, (b) GL modal plane, (c) main lobe peak intensity, and (d) mask transparency in the iterative optimization procedure.

The evolution of the mask phase, the GL modal plane, the main lobe peak intensity, and T with each of the iterations is shown in Fig. 3. While the continuous phase modulations of the mask disappear during the optimization process, the phase singularities remain, suggesting that phase singularities at appropriate locations are principally responsible for the rotation of the PSF. The GL modal plane evolves by picking up different weights for the modes on a cloud around the straight line of the exact rotating PSF. Although the two main lobes were equally boosted by the spatial domain constraint, one of the main lobes (main lobe 1) grows faster than the other main lobe (main lobe 2). Since the constraints in the GL modal plane and in the spatial domain did not preserve the phase-only attribute of the initial estimate, T drops immediately after the first iteration. T eventually increases because of the phase-only constraint in the Fourier domain. After 20 iterations, the main lobe peak intensities and T saturate. We then obtain the phase-only HER-PSF mask [Fig. 1(c)] by stopping the iterative optimization process immediately after applying the phase-only Fourier domain constraint. The HER-PSF has two main lobes that rotate continuously with defocus [Fig. 2(c)] as suggested by its mask's modal decomposition [Fig. 1(f)]. The transfer function efficiency of the exact rotating PSF and the HER-PSF are 1.8% and 56.8%, respectively. Hence, the main lobes of the HER-PSF have over 30 times more energy than the exact rotating PSF. Further, compared to a rotating PSF mask, the HER-PSF mask is easier to fabricate because of its phase-only attribute and also because the phase modulation becomes smoother in the optimization process.

#91135 - $15.00 USD Received 21 Dec 2007; revised 9 Feb 2008; accepted 20 Feb 2008; published 29 Feb 2008

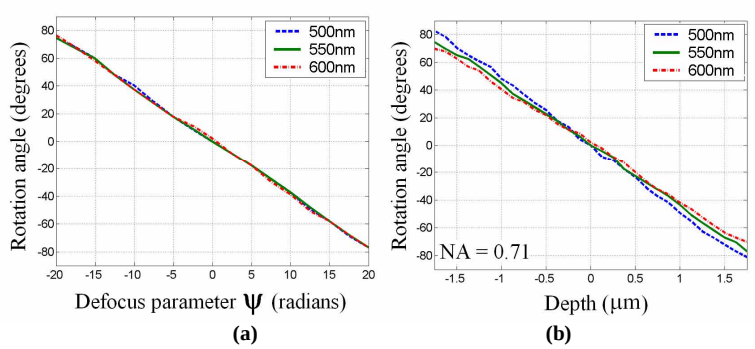

Fig. 4. A HER-PSF mask designed for a wavelength of 550nm, when used with the wavelengths 500nm and 600nm, exhibits (a) same rotation rates as function of defocus parameter (ψ) and (b) slightly different rotation rates as a function of depth (NA=0.71).

Although the HER-PSF design used a coherent transfer function model, it applies equally well for an incoherent imaging system because the incoherent PSF is the modulo-squared of its coherent counterpart. However, because the mask is designed for one particular wavelength, it is interesting to analyze its wavelength (λ) dependence. Wavelength dependence arises from four factors: 1) phase retardation of a mask is $2\pi n\, t(x,y)/\lambda$, where n and $t(x,y)$ are the mask's refractive index and thickness function, respectively; 2) material dispersion; 3) defocus is inversely proportional to λ, and 4) PSF size is inversely proportional to λ. (3) and (4) are the result of diffraction upon wave propagation. As an example, the effect of using a BK7 glass HER-PSF mask designed for a wavelength of 550nm with the wavelengths 500nm, 550nm, and 600nm is shown in Fig. 4. The rotation angles were determined by calculating the 3D PSF for each wavelength from the transmittance function produced by the mask at the corresponding wavelength. For all three wavelengths, the PSF exhibits two main lobes that rotate continuously. The rates of rotation are essentially the same for all three wavelengths [Fig. 4(a)], when plotted as a function of the defocus parameter (ψ), defined in [10]. However, as a function of depth, the rotation rate increases when the mask is used with wavelengths smaller than its design wavelength, and decreases when used with wavelengths greater than the design wavelength. This is exemplified in Fig. 4(b) for a unity magnification system with 0.71 numerical aperture (NA).

For experimental demonstration, we implement HER-PSF with a reflective phase-only spatial light modulator (SLM). Because of the sampling of the phase function by the SLM's pixels, the SLM produces multiple orders, of which the 0^{th} order has the highest energy. In order to avoid on-axis effects due to the SLM's non-ideal modulation, a linear phase is added to the calculated HER-PSF transfer function phase. A collimated light with wavelength 632.8nm is incident on the SLM and a 0.09 NA lens Fourier transforms 0^{th} order of the SLM. The PSF at different axial distances shows two continuously rotating main lobes [Fig. 2(d)] with 37.5% transfer function efficiency. The experimental efficiency is not as high as the theoretical value (56.8%) because of the non-ideal response of the SLM.

6. Conclusion

We introduced HER-PSFs, described their design methodology, analyzed their spatial and frequency response, and demonstrated them experimentally. We showed that HER-PSFs can offer over thirty times higher efficiency than the exact rotating PSFs.

Acknowledgments

S. R. P. Pavani thankfully acknowledges support from a CDM Optics - OmniVision Technologies Ph.D. fellowship. This work was funded by the Technology Transfer Office of the University of Colorado and the National Science foundation (award ECS-225533).

#91135 - $15.00 USD Received 21 Dec 2007; revised 9 Feb 2008; accepted 20 Feb 2008; published 29 Feb 2008